



Factors influencing the accuracy of the photogrammetry-based deformation measurement method

Lin Li¹ · Xiong Zhang²

Received: 26 January 2017 / Accepted: 17 April 2018 / Published online: 14 May 2018
© Springer-Verlag GmbH Germany, part of Springer Nature 2018

Abstract

Triaxial test has been widely used to investigate the stress–strain relationship of unsaturated soils. During triaxial testing, soil volume is an essential parameter to be measured. For an unsaturated soil, due to the presence of air phase, accurate volume/deformation measurement during triaxial testing was a great challenge for researchers. Recently, a photogrammetry-based method has been developed to measure the soil volume/deformation during triaxial testing. Preliminary triaxial test results indicate the new method is simple, accurate, and cost- and time-effective. However, some concerns regarding its measurement accuracy and applicability, which are critical for the dissemination of the photogrammetry-based method, have been raised by other researchers. These concerns were addressed in details in this study. The factors concerning the deformation measurement accuracy were systematically evaluated through a series of triaxial tests on an aluminum cylinder with different confining media and chamber pressures. A sensitivity analysis was carried out to investigate the impact of the system parameters on the volume measurement accuracy of the photogrammetry-based method. In addition, a triaxial test on a saturated sand specimen was conducted to evaluate the influences of mesh density, mesh pattern, and interpolation technique on the volume change measurement accuracy. Finally, some suggestions were provided to improve the accuracy of the photogrammetry-based measurement method.

Keywords Optical ray tracing · Photogrammetry-based method · Triangular mesh · Triaxial test · Unsaturated soil · Volume change

1 Introduction

Triaxial test has been widely used to investigate the stress–strain relationship of both saturated and unsaturated soils. During triaxial testing, soil volume is an essential parameter to be measured. For a saturated soil, its volume change is equal to the water volume change. As a result, the soil volume change can be directly measured through

monitoring the water volume change. However, for an unsaturated soil, due to the presence of air phase, its volume change is no longer equal to the water volume change. As a result, the conventional volume change measurement method for saturated soils cannot be applied to unsaturated soils. In the past few decades, several methods have been developed to measure the soil volume/deformation for unsaturated soils during triaxial testing (e.g., [2, 4–8, 10, 11, 15, 17, 18, 21, 25, 26]). However, as summarized in [16] and [27], all these methods have their limitations and accurate unsaturated soil volume change measurement during triaxial testing remained a great challenge for researchers.

With the development in digital cameras, photogrammetry has been getting more and more attractive for laboratory soil deformation measurement during triaxial testing [12–14, 22, 27] due to its low cost and high measurement accuracy. In [22] and [20], a multi-camera photogrammetric method was proposed to measure the

✉ Lin Li
lli10@alaska.edu
Xiong Zhang
zhangxi@mst.edu

¹ Department of Civil Engineering, University of Alaska Anchorage, Anchorage, AK 99508, USA

² Department of Civil Architecture, and Environmental Engineering, Missouri University of Science and Technology, 135 Butler-Carlton Hall, Rolla, MO 65409, USA

deformation of unsaturated soils during triaxial testing. In this method, 10 pinhole cameras were mounted to the inside of a triaxial chamber. Soil deformation during testing was measured through capturing a series of images around the specimen using the pinhole cameras with the help of a track system. Then, a photogrammetric analysis was performed on the captured images to extract the soil deformation characteristics during testing. The usage of the internal cameras (i.e., cameras inside of the triaxial cell) eliminated the need of refraction correction which was required by the other image-based methods (e.g., [4, 10, 17, 27]). Due to the adoption of photogrammetry, the deformation measurement during triaxial testing was simple and straightforward. However, there are several limitations associated with this multi-camera photogrammetric method: (1) The pinhole cameras used are not commercially available. The user needs to make a selection on existing board cameras and determine the suitable pinhole size for a different triaxial system setup; (2) the pinhole cameras, before each test, needs to be saturated to eliminate the refraction due to the air inside the camera body. This camera saturation process is considered to be very critical for an accurate soil deformation measurement; (3) a significant system modification on the existing triaxial test apparatus is required for the camera installation (i.e., build two camera towers) and image capturing (i.e., build a track system and a data acquisition system). As a result, the system setup required by the multi-camera photogrammetric method was more complicated than all other image-based methods; (4) the captured images are in very poor quality due to the low resolution of the pinhole camera. Therefore, the accuracy of the photogrammetric measurement using blurry images is questionable. Since each image only covers a small area of the specimen, hundreds of images are required for a single volume measurement; and (5) the multi-camera photogrammetric analysis using hundreds of images captured by 10 cameras with different calibration results is extremely complicated and time-consuming as reported in [20]. Due to the above-mentioned limitations, accurate soil deformation measurement during triaxial testing using this multi-camera photogrammetric method is neither practical nor efficient even though the measurement principle is theoretically sound.

1.1 A photogrammetry-based method

A novel photogrammetry-based method [12, 14, 27, 28] has been developed and successfully applied to measure the soil volume/deformation during triaxial testing. The photogrammetry-based measurement is achieved through accurate determination of each optical ray from the corresponding camera station to the measurement target on the soil surface inside the triaxial cell. The principle of the

photogrammetry-based method is schematically shown in Fig. 1.

To measure the volume of an unsaturated soil specimen during triaxial testing using the newly developed photogrammetry-based method, a series of images (typically between 25 and 30) are captured for the conventional triaxial testing system using a hand-held digital camera. Images can be taken from any arbitrary directions or shooting angles as long as the adjacent images have sufficient overlap as typically shown in Fig. 1a. The camera stations where the images are taken and the geometric properties of the triaxial cell are accurately determined through a photogrammetric analysis. With the pixel positions of points on the images, the corresponding optical rays from each camera station to the cell surface are constructed as typically shown in Fig. 1a. When these optical rays reach the cell surfaces (i.e., outer and inner surfaces), they change their directions due to refraction. The Snell's law is then adopted to accurately calculate the directions of the optical rays after refractions at the air–cell and cell–fluid interfaces as shown in Fig. 1b. For a specific measurement target “*P*” on the soil surface, multiple optical rays from different camera stations can be constructed. Subsequently, the three-dimensional (3D) coordinates of the point are determined through a least-square estimation technique using the optical rays after the refraction at the cell–fluid interface as shown in Fig. 1c. With the 3D positions of all the targets on the soil surface at different loading steps, the soil deformation characteristics during loading can then be extracted as typically presented in [14].

The newly developed photogrammetry-based method is significantly different from all other image-based methods as summarized in [14]. The major advantage of the photogrammetry-based method is that no modification on the triaxial system is required for soil volume/deformation measurement. As a result, other than the complicated double-walled cell triaxial system, the conventional triaxial cell, designed to test saturated soils, can be directly used to characterize unsaturated soils which is in great significance for the laboratory tests on unsaturated soils. Besides the volume measurement, this method was also capable of measuring the full-field strain distribution, volumetric strain non-uniformity, strain localization, 3D bulging, and shear plane evolution of soils during triaxial testing [14]. Preliminary triaxial test results, as reported in [27] and [14], indicate that the photogrammetry-based method is simple, accurate, and cost- and time-effective. The average point and volume measurement accuracies were evaluated to be approximately 0.07 mm and 0.1%, respectively. However, some concerns were raised regarding the accuracy and applicability of the method and possible problems during the ray tracing process as presented in [23]. These concerns were briefly addressed in [28] without extensive

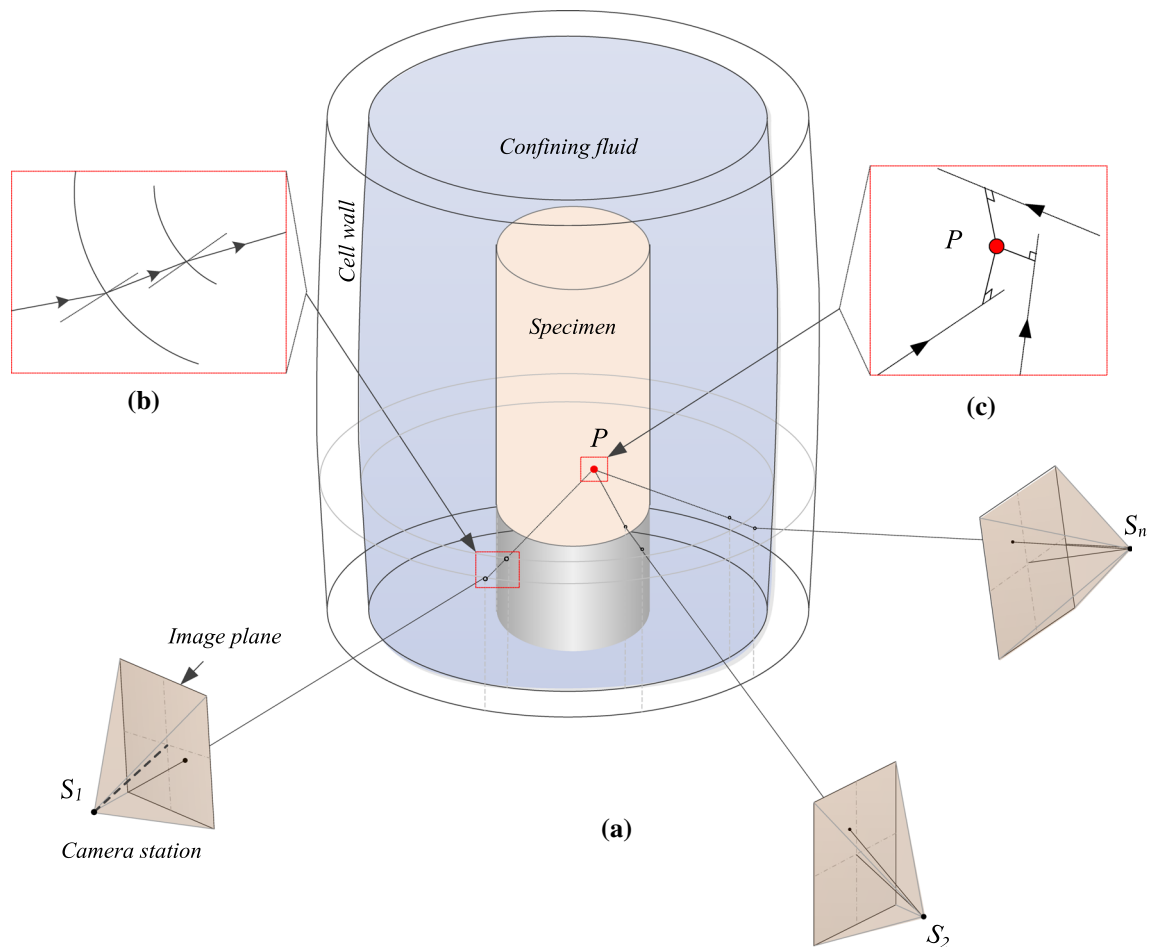


Fig. 1 The photogrammetry-based method (modified from Li et al. [13]): **a** system setup; **b** Snell's law; and **c** least-square estimation

experimental evidence. Some system parameters such as the acrylic cell size and the cell wall thickness, which vary in different triaxial test apparatus, indeed have influences on the measurement accuracy. These influences have never been thoroughly investigated since the proposed photogrammetry-based method is still very new. In addition, the photogrammetry-based method was developed for the purpose of measuring the deformation of unsaturated soils during triaxial testing. Besides water, in some cases, air, silicone oil, and some other fluids could also be used as the confining medium in triaxial tests (e.g., AASHTO T307 [1], ASTM D7181 [3, 22]). The use of a different confining medium can result in a change in the refractive index which inevitably affects the accuracy of the optical ray tracing process. As a result, the impact of the refractive index of the confining medium on the measurement accuracy needs to be evaluated. In the previous study [14], the soil volume was calculated through triangular meshes generated using the measurement targets on the soil surface. The influences of the mesh density, mesh pattern, and interpolation technique on the accuracy of the soil volume

measurement were also questioned by some researchers [23] and have never been evaluated. Therefore, there is a great need to further evaluate the accuracy and influence factors of the photogrammetry-based method when used for triaxial deformation measurements.

A series of tests on an aluminum cylinder under different confining medium and chamber pressure conditions were performed in this study to: (1) evaluate the point measurement accuracy of the photogrammetry-based method under different confining media (i.e., air, water, and silicone oil); (2) evaluate the impact of the system parameters (i.e., refractive indices of air, cell wall, and confining fluid and the thickness of the triaxial cell wall) on the overall volume measurement accuracy; and (3) further address the problems regarding the photogrammetry-based method raised by Salazar and Coffman [23]. In addition, a drained triaxial test on a saturated sand specimen was performed to evaluate the influence of mesh density, mesh pattern, and interpolation technique on the overall volume measurement accuracy. Finally, some suggestions are

provided to improve the accuracy of the photogrammetry-based method.

2 Evaluation tests on an aluminum cylinder

2.1 Specimen preparation and triaxial testing

An aluminum cylinder (71 mm in diameter and 142 mm in height, which is consistent with a typical triaxial soil sample size), as shown in Fig. 2a, was fabricated to evaluate the point and volume measurement accuracy of the photogrammetry-based method. A total number of 260 measurement targets (20 targets/circle \times 13 circles) were posted to the cylinder surface to facilitate the measurements and the following analysis. An acrylic cell used in this study, as shown in Fig. 2b–d, was 304 mm in height, 165 mm in outer diameter, and 9.70 mm in thickness with a refractive index of 1.491. A total number of 324 measurement targets (in 6 circles (45 targets/circle) and 3 vertical stripes (18 targets/strip), which would be used to determine the camera stations and reconstruct the cell wall, were posted to the outer surface of the acrylic cell.

The experimental program included measuring the 3D positions measurement targets on the aluminum cylinder surface under the following conditions: (1) exposed in air as shown in Fig. 2a and (2) installed in the triaxial cell as shown in Fig. 2b–d under 0, 200, 400, and 600 kPa chamber pressures with air, water, and silicone oil as the confining media. Since the modulus of elasticity of aluminum is 69 GPa, it was reasonable to assume the aluminum cylinder to be rigid under a confining pressure less than 600 kPa. As a result, the 3D positions of the measurement targets on cylinder surface measured using the

photogrammetric technique before the installation of the triaxial cell provided a good reference for measurement accuracy evaluation. The tests were performed according to the following procedure: (1) firmly fix the aluminum cylinder on the pedestal of the triaxial cell; (2) capture approximately 25 pictures images to extract the 3D position of the targets on the cylinder surface; (3) carefully install the triaxial cell; (4) capture images at different chamber pressures (i.e., air pressure at 0, 200, 400, and 600 kPa); (5) release the air pressure in the cell and then slowly fill up the cell with water; (6) capture images at different chamber pressures (i.e., water pressures at 0, 200, 400, and 600 kPa); (7) drain the water out and fill the cell with silicone oil; and (8) capture images from different orientations at different chamber pressures (i.e., oil pressures at 0, 200, 400, and 600 kPa).

2.2 Cell wall deformation under pressure

Typical images of the triaxial chamber with different confining media (i.e., air, water, and silicone oil) are presented in Fig. 2b–d. It is interesting to find that the diameter of the same aluminum cylinder appeared to be different in the same triaxial cell when filled with different confining media. The aluminum cylinder in the air-filled chamber appeared to be much smaller than that in the chamber when filled with water or silicone oil. This was because the cell surface was curved in the circumferential direction and the refractive indices of air (i.e., 1.000), water (i.e., 1.339), and silicone oil (i.e., 1.407) were different from each other. The higher the refractive index, the larger the distortion of the specimen in the radial direction. Meanwhile, the height of the cylinder appeared to remain

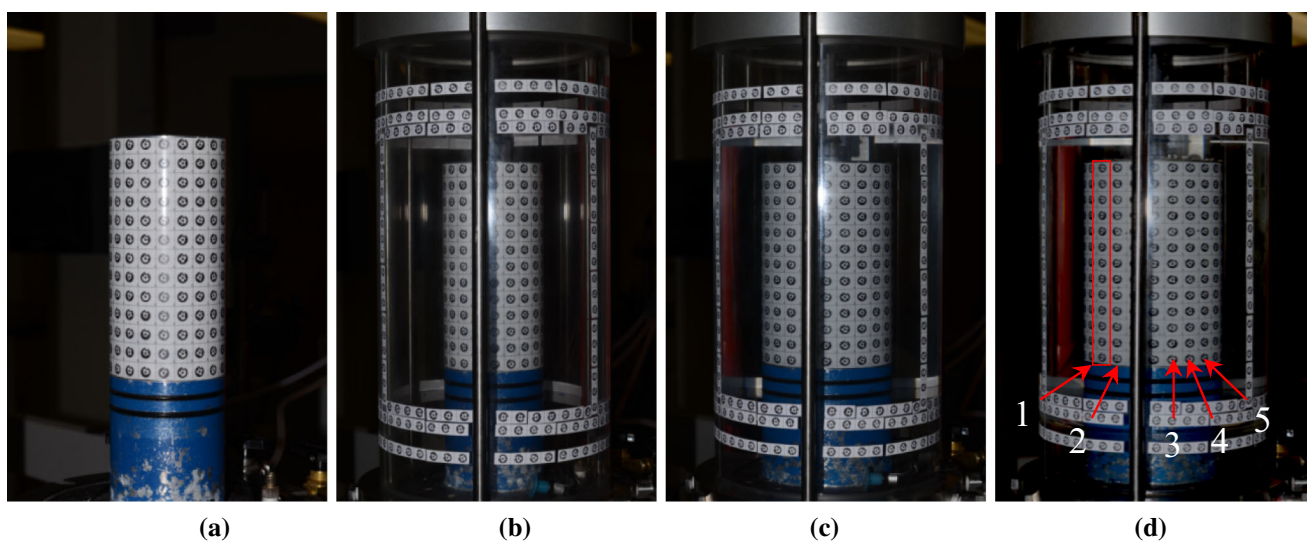


Fig. 2 Evaluation tests on the aluminum cylinder: **a** in air; **b** in air-filled chamber; **c** in water-filled chamber; and **d** in silicone oil-filled chamber

the same as shown in Fig. 2b–d because the cell surface was relatively straight in its axial direction.

With the images captured after the cell installation, a photogrammetric analysis was performed to determine the camera stations where the images were captured. A typical example of the camera stations is shown in Fig. 3a in which a total number of 30 images were captured around the triaxial system at 0 kPa chamber pressure when the silicone oil was used as the confining fluid. The camera stations were labeled as “CS”. Besides this, the 3D positions of the targets on the surface of the acrylic cell wall were also determined with known camera stations. With these targets, the locations of the acrylic wall could be determined. The acrylic was assumed to be barrel shaped, and the maximum cell wall radii under different chamber pressures and confining medium conditions were obtained through a least-square method as described in [27] and plotted against the chamber pressure as shown in Fig. 3b. With increasing chamber pressure, the radius of the triaxial cell continually increased from 82.98 to 83.10 mm under air-, water-, and oil-filled chamber conditions. With the applied chamber pressure and the thickness and radius of

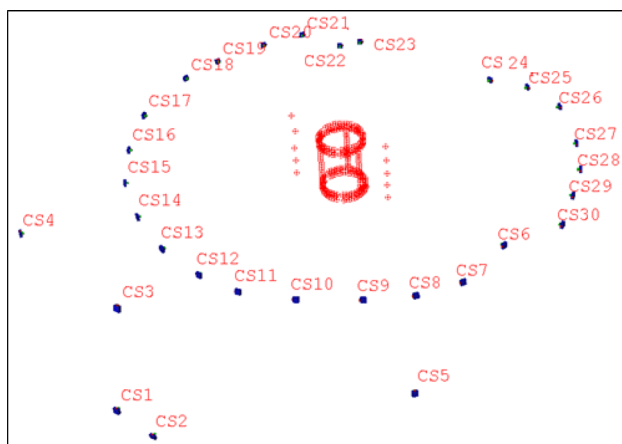
the cell wall, the hoop stress in the acrylic cell was calculated using the following equation:

$$\sigma_{\theta} = \frac{P \cdot r}{t} \quad (1)$$

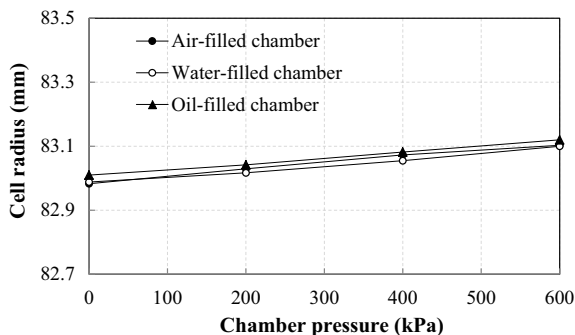
where P = internal chamber pressure, t = acrylic cell wall thickness (i.e., 9.7 mm), r = mean radius of the triaxial cell, and σ_{θ} = circumferential or hoop stress.

The hoop stress under different chamber pressures was calculated and is listed in Table 1. Under a chamber pressure of 600 kPa, the hoop stress (in tension) in the cell wall was 4.84 MPa which was much less than the yield strength of acrylic (i.e., 70 MPa). As a result, the response of cell diameter was nearly linear (i.e., elastic) as shown in Fig. 3b. With the hoop stress and the Young’s modulus of 3.2 GPa, the theoretical strain in the acrylic cell wall under different chamber pressures was calculated and is listed in Table 1. Besides this, the strain in the acrylic cell wall was also calculated based on the variation of cell radius under different chamber pressure and confining medium conditions as summarized in Table 1. The strain measured in the acrylic cell wall was in agreement with the calculated strain which indicated that the cell radius variation under different chamber pressures, which was neglected in all other image-based methods, could be captured by the photogrammetry-based method.

Using the images captured before the installation of the triaxial cell, the 3D coordinates of the measurement targets on the cylinder surface were measured through photogrammetric analyses at an accuracy of 0.01 mm as evaluated in [27]. Besides this, with the 3D coordinates of the measurement targets on the cylinder surface, assuming to be deformable and barrel shaped, the orientation of the cell wall under different confining fluid and pressure conditions was reconstructed. Then, the 3D positions of the targets on the cylinder surface were determined through the optical ray tracing and least-square estimation techniques. Since the optical ray tracing process in a 3D space according to the Snell’s law, which is a theoretical equation instead of an empirical one, the accuracy of the photogrammetry-based measurement was supposed to be equal



(a)



(b)

Fig. 3 Triaxial test under different chamber pressure and confining medium conditions: **a** camera station for image capturing; **b** cell radius variation

Table 1 Theoretical and measured strain of the acrylic cell wall

Chamber pressure (kPa)	Hoop stress (kPa)	Strain (%)	Measured strain (%)		
			Air-filled	Water-filled	Oil-filled
0	0	0.000	0.000	0.000	0.000
200	1612	0.050	0.056	0.035	0.039
400	3226	0.101	0.109	0.080	0.087
600	4840	0.151	0.145	0.135	0.133

or at least comparable to the accuracy of the photogrammetric method (i.e., 0.01 mm). However, this was not the truth according to the measurement results presented in previous studies (i.e., [14, 27] in which the accuracy of the photogrammetry-based method used in multi-media was much lower than that of the photogrammetric measurement in one medium condition. It should be noted that this accuracy reduction was a result of coupling effect of several factors such as assumptions on triaxial cell wall, and refractive indices of the cell and confining medium. These influence factors were carefully evaluated as follows.

2.3 Influence of assumptions on triaxial cell wall

To facilitate the photogrammetry-based analysis and the optical ray tracing process, the refractive indices used for air, cell wall, water, and silicone oil under different pressures (i.e., 0–600 kPa) were 1.000, 1.491, 1.339, and 1.407 which were determined through a least-square estimation. With the 3D coordinates of the targets on the cylinder surface measured under different conditions (i.e., exposed in the air and in the triaxial cell filled with air, water, and silicone oil), a comparison of point measurement accuracy was made between the results obtained from the photogrammetric (i.e., before installation of the triaxial cell) and photogrammetry-based (i.e., after installation of the triaxial cell) analyses as shown in Fig. 4. The measurement accuracy at different chamber pressure and confining medium conditions was represented by the color of the points. The overall point measurement error of the photogrammetry-based method when water (Fig. 4b) or silicone oil (Fig. 4c) was used as the confining medium was less than that of the air-filled cell condition (Fig. 4a). At different chamber pressure and confining medium conditions, the high measurement error was always found to be at the right side of the cylinder and the low error was at the left side. Also, for the same confining medium, the error distribution patterns under different chamber pressures were similar to each other as shown in Fig. 4a–c. The reasons for this repeatable error distribution pattern were attributed to: (1) the assumption on the cell surface which was best fitted by an equation represented a barrel-shaped surface. Using the targets at the bottom circle (see Fig. 2b) as an example, Fig. 5a presents the distances (i.e., fitting error) between those targets and the reconstructed cell surface. The error distribution indicated that the cross section of the triaxial cell was slightly elliptical rather than circular; and (2) the assumption of a uniform thickness (i.e., 9.7 mm) was not consistent with the real cell wall thickness which varied from 9.40 to 9.89 mm according to digital caliper measurement results. Figure 5b presents the thickness of the cell wall at different locations which showed that the upper left side of the cell was slightly

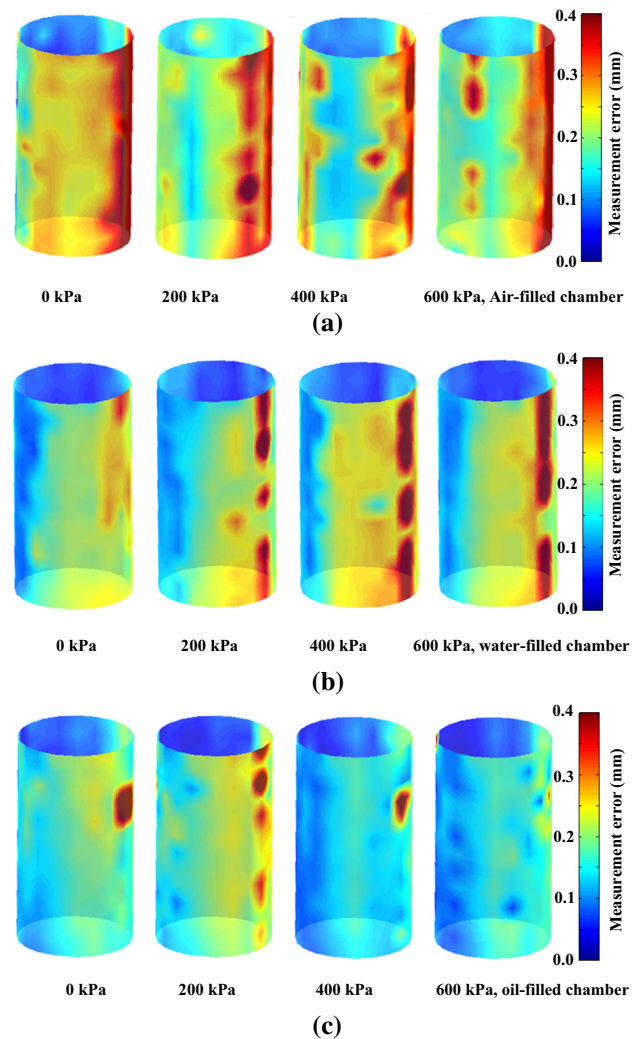


Fig. 4 Point measurement error distribution

thicker than the lower right side. Due to the geometrical imperfection of the cell, the assumptions on cell wall shape and thickness inevitably resulted in errors in the optical ray tracing process and the subsequent point measurement results. Consequently, the measurement accuracy of the photogrammetry-based method was dependent on the representativeness of the equation for the cell surface. To be specific, if the cell surface was assumed to be cylindrical or barrel shaped, the accuracy was highly dependent on the cell roundness and uniformity in thickness. With a higher machining accuracy (cylindrical with a uniform thickness), the accuracy of the photogrammetry-based method could be definitely improved.

The point error (i.e., distance between the points measured by the photogrammetric analysis and photogrammetry-based analysis) was used as a statistical measure of the accuracy to of the photogrammetry-based method. These point measurement errors under different confining medium conditions are summarized in Table 2. The overall

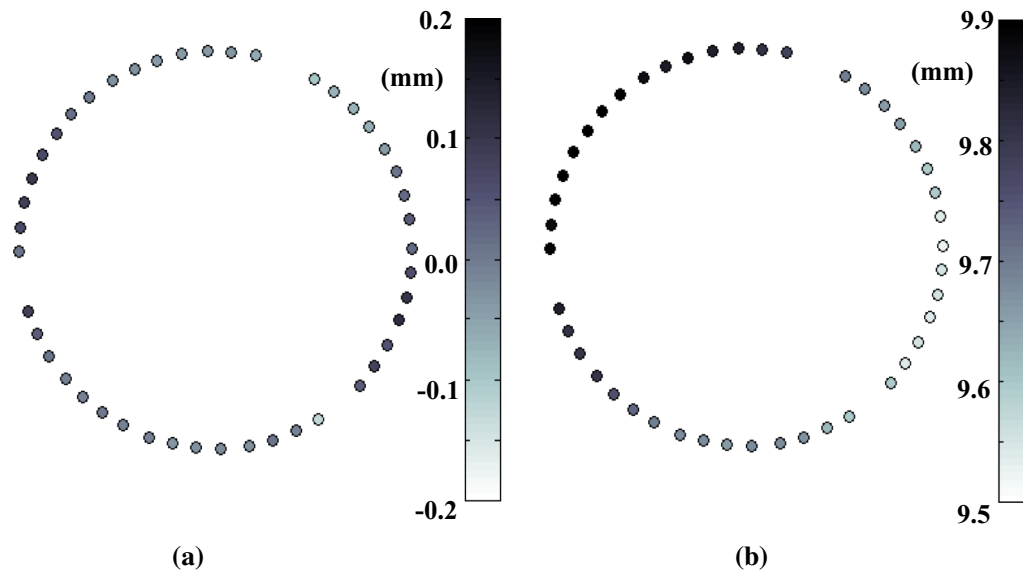


Fig. 5 Cell wall reconstruction: **a** distance between the targets and the reconstructed cell wall surface and **b** cell wall thickness at different locations

Table 2 Point measurement accuracy

Confining medium	Cell pressure (kPa)	0	200	400	600
	Point measurement accuracy (mm)				
Air	Average	0.210	0.208	0.197	0.213
	STD	0.141	0.098	0.120	0.123
Water	Average	0.138	0.137	0.161	0.147
	STD	0.080	0.089	0.103	0.099
Water _{rigid cell}	Average	0.140	0.140	0.160	0.144
	STD	0.079	0.089	0.102	0.099
Oil	Average	0.136	0.149	0.114	0.117
	STD	0.077	0.095	0.059	0.068

point measurement error increased from 0.01 mm (i.e., accuracy of the photogrammetric method as reported in [27]) to 0.13, 0.15 and 0.21 mm when silicone oil, water, and air were used as the confining medium. Compared with the average point measurement error of 0.07 mm as presented in [27] when water was used as the confining fluid, the accuracy obtained in this study was nearly doubled or tripled for the water- and oil- and the air-filled chamber conditions, respectively. Besides the influence of the assumption on cell wall, one of the major reasons for this was the triaxial cells used were different. In [27], a 101.6 mm in diameter acrylic cell was used, while in this study, the acrylic cell used was 166 mm in diameter. As indicated in the previous study, the thickness of the older acrylic cell was not uniform as well. The measurement error during the optical ray tracing process would be

magnified with an increase in the optical ray traveling distance due to the error induced by the imperfection of the cell wall. This problem can, however, be easily solved by using a better acrylic cell at relatively low cost.

In the other image-based methods (e.g., [4, 10, 15, 17]), the cell wall was assumed to be perfectly rigid and cylindrical which is different from the assumption of deformable and barrel shaped used in the photogrammetry-based method. The assumption of a rigid and cylindrical cell was not consistent with the real cell shape and would inevitably introduce error to the measurement. To evaluate the influence of this assumption on the overall point measurement accuracy, the optical ray tracing analysis was also performed with an assumption of a perfectly cylindrical cell with constant thickness and diameter. Using the measurement when the chamber was filled with water as an example, the measurement difference between using the perfectly cylindrical cell and deformable barrel-shaped cell surface was well below 0.01 mm according to the results summarized in Table 2 which was considered to be negligible for triaxial soil deformation measurement. It seems the small protrusive deformation in the vertical direction at the center of the acrylic cell has little influence on the accuracy of the measurement. However, it should be noted that this conclusion is valid only when the following conditions are satisfied: (1) The cell wall surfaces are accurately reconstructed; (2) the cell deformation under pressure is negligible; and (3) multiple rays from different camera stations are used for the measurement of a single point. In the conventional image-based methods (e.g., [4, 10, 15, 17]), the triaxial cell position was manually controlled, the cell deformation under pressure was

unknown, and only one optical ray was used for the measurement of a single point on the soil surface. In other words, none of the above conditions was satisfied in the conventional image-based methods. Using the camera station 10 as shown in Fig. 3a as an example, the influence of an inaccurate cell position on the point measurement accuracy was analyzed as follows.

To be consistent with the conventional image-based methods (e.g., [4, 10, 15, 17]), a 2D coordinate system was built as shown in Fig. 6. The corresponding image at camera station 10 is shown in Fig. 2d. There were five columns of targets that can be clearly identified as shown in this image. With the photogrammetry-based method, the cell position and shape as well as the camera station were accurately reconstructed based on the principle of photogrammetry (e.g., [12, 14]). The optical rays for those targets were then constructed from the corresponding camera station to the cylinder surface after refractions as typically shown in Fig. 6. Meanwhile, the incident angles, φ_1 and φ_2 at the air–cell and cell–oil interfaces for the optical ray tracing process were calculated and are summarized in Table 3. For the same optical ray, the φ_1 was always greater than φ_2 due to the refraction at the air–cell interface. Since the measurement targets on the cylinder surface were accurately measured using the photogrammetric method before the installation of the triaxial chamber, the point measurement error in x -axis direction (the distance between the point “ p ” and the corresponding

optical ray as shown in Fig. 6) was also determined as shown in Table 3. The average error for the targets in five columns was generally within 0.05 mm in x -axis direction. To simulate an inaccurate cell position, the reconstructed cell surface was then shifted ± 1 mm along the x -axis direction. Subsequently, the optical ray tracing process was performed using the shifted cell surface. The incident angles and error obtained were also summarized in Table 3. A shift of the reconstructed cell surface along x -axis direction caused a slight increase or decrease in the incident angles depending on the shift direction. Also, a significant increase in the measurement error from 0.01 mm to approximately 0.234 mm was identified for the targets in column 1 due to the change in incident angles.

The comparisons made above indicated that the proposed photogrammetry-based method has good tolerances for non-perfect testing conditions since the camera orientations and location of the acrylic cell accurately determined by photogrammetry and the coordinates of the measurement points were obtained from least-square optimization using multiple optical rays from different camera stations. In contrast, the accuracy of the conventional image-based methods highly depends on whether the assumptions made are satisfied. Those conditions in reality are very difficult to meet, and a small deviation from the assumed conditions will lead to unacceptable errors.

2.4 Influence of cell wall cleanliness

One concern raised by Salazar and Coffman [23] was the measurement accuracy of the photogrammetry-based method can be influenced by the cleanliness of the cell wall. In the photogrammetry-based method, for a single image as typically shown in Fig. 2d, many optical rays could be constructed and traced from the corresponding camera station to the cylinder surface as shown in Fig. 7a which clearly shows that some of optical rays to the cylinder surface were missing as indicated by the gap between optical rays. This was because of the frame rod and its shadow, as shown in the corresponding image (i.e., Fig. 2d), blocked the light ray to some of the targets on the cylinder surface. Besides the frame rod, the optical rays to the cylinder surface could also be blocked by the targets or stain on the cell surface or covered by the white reflection area due to camera flash. However, for the photogrammetry-based method, at least three images were used to measure the 3D position of a single target. As long as the target on the cylinder surface could be “seen” on the other images, its 3D position could still be accurately determined using the least-square estimation technique. As a result, the concern regarding the cleanliness or geometrical imperfections of the acrylic cell raised by Salazar and Coffman [23] was not a problem at all. This is because the stains are

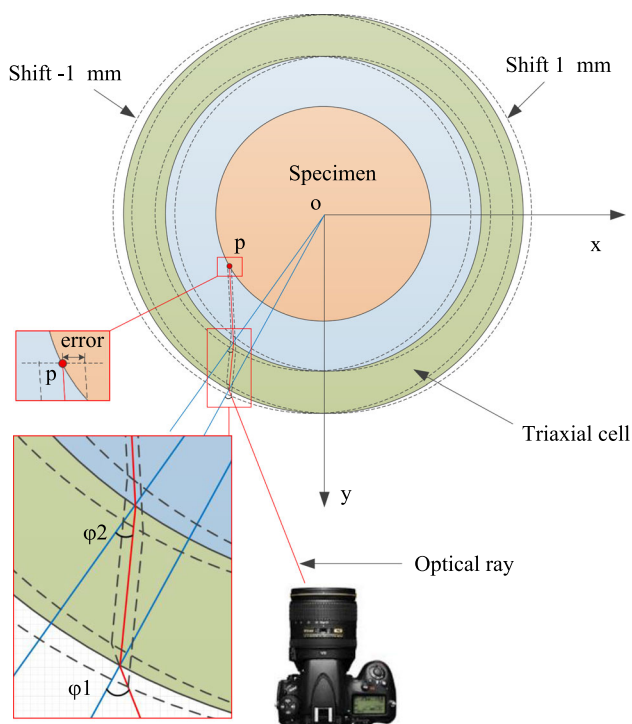
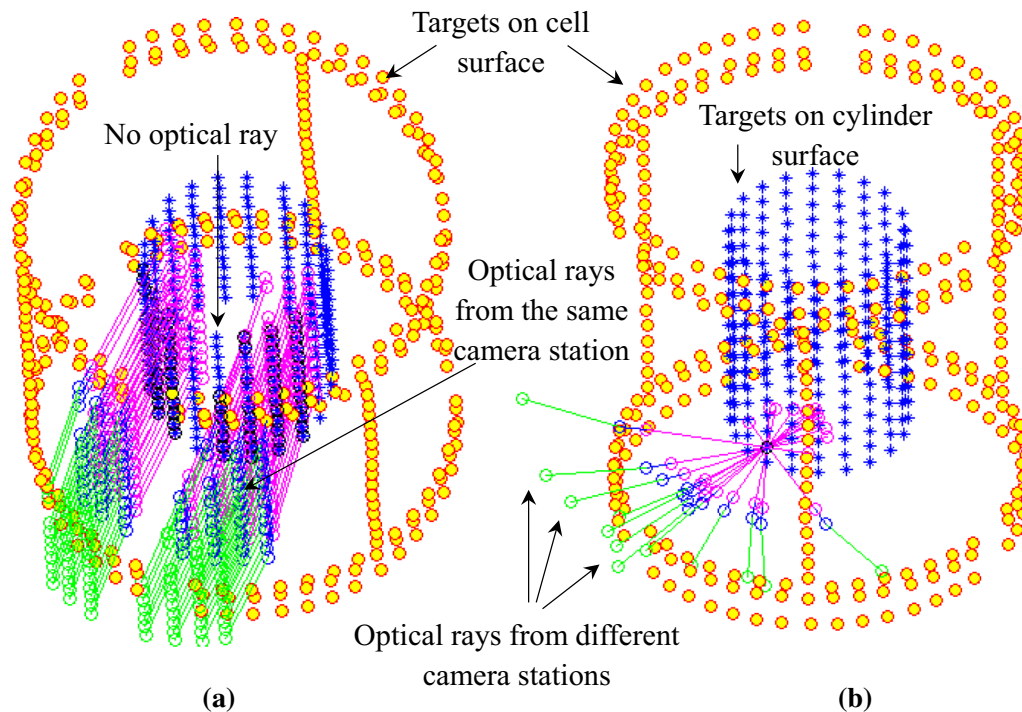


Fig. 6 Measurement error due to inaccurate cell position

Table 3 Measurement error due to inaccurate cell positions

Column	φ_1 (°)			φ_2 (°)			Error (mm)		
	Shift 0	+ 1 mm	– 1 mm	Shift 0	+ 1 mm	– 1 mm	Shift 0	+ 1 mm	– 1 mm
1	27.75	27.11	28.39	20.65	20.19	21.12	0.010	0.234	– 0.217
2	19.92	19.31	20.52	14.92	14.47	15.37	0.010	0.204	– 0.187
3	9.57	10.13	9.02	7.12	7.55	6.69	0.009	0.117	– 0.131
4	18.30	18.92	17.68	13.71	14.18	13.25	0.009	0.102	– 0.108
5	26.30	26.97	25.63	19.61	20.09	19.12	– 0.045	0.044	– 0.140

**Fig. 7** Ray tracing process: **a** ray tracing from one camera station; **b** ray tracing to a single target from different camera stations

just like the targets posted on the acrylic wall which can only block the light to the cylinder surface at certain angle. Figure 7b shows a typical optical ray tracing process for a single target on the cylinder surface. This target was identified on 12 different images and not “seen” in the rest of more than a dozen images. However, it does not have any impact on the proposed photogrammetry-based method. As shown in Fig. 7b, a total number of 12 light rays were constructed and traced to the cylinder surface. The 3D position of this target could still be accurately determined even though some of those 12 light rays were missing (i.e., blocked by the frame rod, the targets and stain on the cell surface, or the white area caused by camera flash).

2.5 Influence of confining media refractive index

In this section, the volume measurement accuracy was utilized to evaluate the influences of the refractive index of the confining medium. To calculate soil volume, the triangular meshes were generated using the targets on the cylinder surface. The corresponding cylinder volumes at different chamber pressure and confining medium conditions were calculated as shown in Fig. 8 using the method presented in [14].

Since the point measurement accuracy of the photogrammetric method in the air was very high [27], it is reasonable to assume the volume measurement results of the aluminum cylinder when exposed in air to be the “true” volume. Comparing with this volume, the average volume measurement accuracy (defined as the measurement error divided by the cylinder volume) of the photogrammetry-

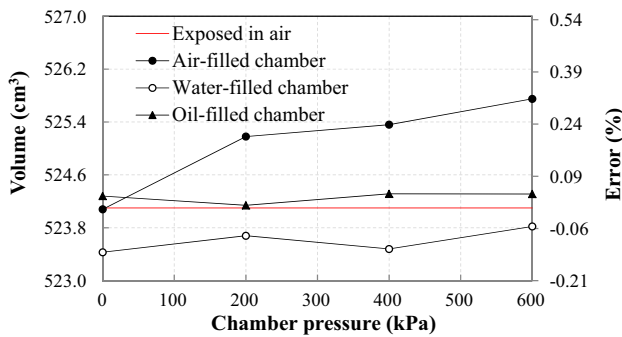


Fig. 8 Cylinder volumes measured under different chamber pressure and confining medium conditions

based method was 0.092 and 0.03% when water and silicone oil were used as the confining medium, respectively. The volume measurement accuracy also did not vary significantly at different chamber pressures.

As shown in Fig. 8, when the air was used as the confining medium, the volume measurement accuracy was lower than that of the water- or oil-filled cell condition with chamber pressure greater than 200 kPa. The major reason for this measurement accuracy variation was attributed to the refractive indices of air, water, and silicone oil. It is well known that a material refractive index will vary with the light wavelength (e.g., [9]). A change in the lighting condition, which means a change in the wavelength of light, can result in a change of refractive index. Waxler and Weir [24] reported that the water refractive index would change at different pressure and temperature conditions. A pressure change from 0 to 25,832 kPa resulted in a change of water refractive index from 1.33423 to 1.33805 at 7.64 °C under the same lighting condition. In this study, all tests were conducted at a nearly constant room temperature of 23 °C. The chamber pressure only varied from 0 to 600 kPa. The camera built-in flash was used as the light source for all tests. As a result, it was reasonable to assume a constant refractive index of water during triaxial testing. The refractive index of the silicone oil used was also assumed to be constant since no evidence showed that its refractive index would vary with pressure. As presented in Fig. 8, no significant volume measurement accuracy variation was identified when water or silicone oil was used as the confining liquid which verified the rationality of the assumption on the refractive indices of water and silicone oil. However, unlike water and silicone oil, according to Owens [19] and Edlén [9], the refractive index of air would increase with increasing pressure and decreasing humidity and temperature. Since the refractive indices of air under a pressure ranging from 0 to 600 kPa at the room temperature were not exactly known, the air refractive index was also assumed to be constant for the optical ray tracing process in this study. The assumption of a constant air

refractive index resulted in an increase in volume measurement error from 0.0 to 0.31% when chamber pressure increased from 0 to 600 kPa as presented in Fig. 8. However, this relatively high measurement error at a chamber pressures greater than 400 kPa didn't necessarily mean that the air could not be used as the confining media for the triaxial test. Theoretically, as long as the accurate refractive indices of air at different pressure, humidity, and temperature conditions were known, the accuracy of the photogrammetry-based method can definitely be improved for the air-filled chamber condition. Since the volume of the cylinder was accurately determined through the photogrammetric method when exposed in the air, this volume was utilized to best-estimate the refractive index of air at chamber pressures of 200, 400, and 600 kPa through the least-square method. This best estimation was performed by minimizing the difference between the measured volumes at different air-filled chamber pressure and exposed in air conditions through varying air refractive indices. The corresponding best-fit air refractive indices at chamber pressures of 200, 400, and 600 kPa were determined to be 1.0017, 1.0019, 1.0025, respectively. The increase in air refractive index because increasing pressure is consistent with the findings presented in [19] and [9].

2.6 Sensitivity analysis

When using the photogrammetry-based method to measure soil deformation during triaxial testing, besides the assumption on the cell shape, some system information including camera information, acrylic cell wall thickness, refractive indices of confining medium and acrylic cell wall is also required for the optical ray tracing process. Camera information which includes image sensor size, pixel numbers, focal length, and several distortion parameters can be accurately determined through camera calibration as presented in [27]. The acrylic cell wall thickness, refractive indices of the confining fluid and acrylic cell wall are three external parameters which can influence the accuracy of the photogrammetry-based measurement. Using the cell filled with water as an example, a sensitivity analysis was performed to clarify the influence of three parameters on the overall volume measurement accuracy. The refractive indices used for water (i.e., n_w) and triaxial cell wall (i.e., n_c) were 1.339 and 1.491, respectively. The cell wall thickness used was 9.70 mm. For the sensitivity analysis, a specific range (i.e., 1.336–1.342 for water refractive index " n_w ", 1.488–1.494 for cell wall refractive index " n_c ", and 9.40–10.00 mm for cell wall thickness " t ") was assigned to each parameter. To eliminate the coupling effect, each time, one of three parameters was set to be a variable and the other two parameters remained to be constants. The sensitivity analysis results are presented in Fig. 9 where the

abscissa scale is different for each parameter with its values shown in the legend.

As can be seen in Fig. 9, the measured cylinder volume decreased with an increase in cell wall thickness, water and cell refractive indices. Since the thickness of cell was much less than the “thickness” of water (i.e., distance between the cell inner surface and the cylinder surface), the refractive index of water has the most significant impact on the overall volume measurement accuracy when comparing with the other two parameters.

3 Evaluation test on a saturated sand specimen

3.1 Specimen preparation and triaxial testing

To accurately measure the volume change of a deforming soil, besides the accurate determination of the system parameters as discussed above, the number of the measurement targets on the soil surface is also considered to be critical. A drained triaxial shearing test was performed on a saturated sand specimen to further evaluate the volume measurement accuracy of the photogrammetry-based method. The same triaxial cell used for the tests on the aluminum cylinder was also used for the sand specimen. Oven dried fine sand (particle size ranging from 0.075 to 0.425 mm) was used to fabricate a sand cylinder (71 mm in height and 126 mm in diameter). After compaction, the sand specimen was carefully mounted to the pedestal of the triaxial cell. A 50 kPa vacuum pressure was applied to hold the sand specimen in place during sealing. A total number of 252 measurement targets (21 targets/circle \times 12 circles) were then posted to the membrane which covered the sand specimen as shown in Fig. 10a. Two circles of measurement targets were posted on the top cap, and the pedestal to ensure the volume change of the specimen was covered by the measurement targets as shown in Fig. 10a. The triaxial cell was installed and filled with tap water after posting the measurement targets. The saturation process was consistent

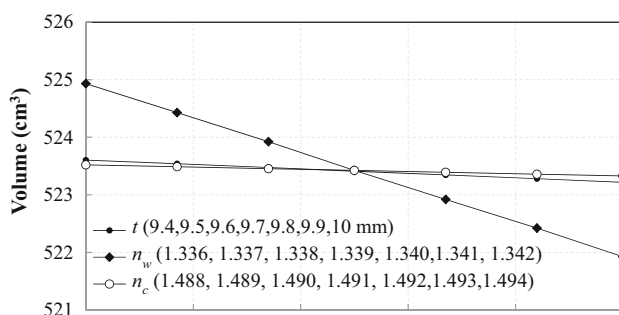


Fig. 9 Sensitivity analysis results

with that presented in [27]. When a B value of 0.95 was reached, the sand specimen was considered to be saturated. The de-aired water was then allowed to enter the saturated sand specimen from the bottom to replace the original water, which was air rich and would suffer from water cavitation problem. Drained triaxial shearing test was then performed after this water replacement.

A vertical displacement rate of 0.2 mm/min was applied to the saturated sand at a net confining pressure of 50 kPa. During loading, drainage valve was kept open to allow water exchange. The volume change of the specimen was recorded by monitoring the amount of water exchange. At different vertical displacement levels (i.e., 0, 2, 4, 6, 8, 10, 13, 16, and 20 mm), the drainage valve was shut off to ensure there was no soil volume change during the subsequent image capturing process. For each volume measurement, approximately 25 images were captured. The validation test was stopped when a total displacement of 20 mm was reached. Figure 10a–c shows the images of the specimen at axial displacement levels of 0, 10, and 20 mm, respectively. The 3D coordinates of the measurement targets on the soil surface at different axial displacement levels were obtained using the photogrammetry-based method. The triangular meshes were then built using the 3D position of those targets at different axial displacements as shown in Fig. 11. The soil specimen was cylindrical at the initial stage, and there was no obvious change in soil shape when the axial displacement reached 2 mm. With increasing axial displacement, the soil specimen gradually bulged into barrel shaped which was consistent with the pictures as shown in Fig. 10. This shape variation was reasonable since the friction between the soil specimen and the loading platens (or pedestal) restrained the soil from deforming along the radial direction at both ends.

3.2 Test results and data analysis

The volume changes of the soil specimen were recorded using the conventional method through monitoring the water exchange and the photogrammetry-based method based on the obtained triangular meshes as shown in Fig. 11. A volume change comparison between two methods at different axial displacement levels is presented in Fig. 12. Both results indicated that the soil volume continuously increased with an increase in the axial displacement. The measurement results from two methods matched well except a slight variation at the axial displacements of 10 and 13 mm.

The soil volume changes of the saturated sand specimen were calculated based upon the obtained triangular mesh. Different meshes could be generated if the number of the measurement targets for mesh generation was different. As a result, different volume change results were expected due

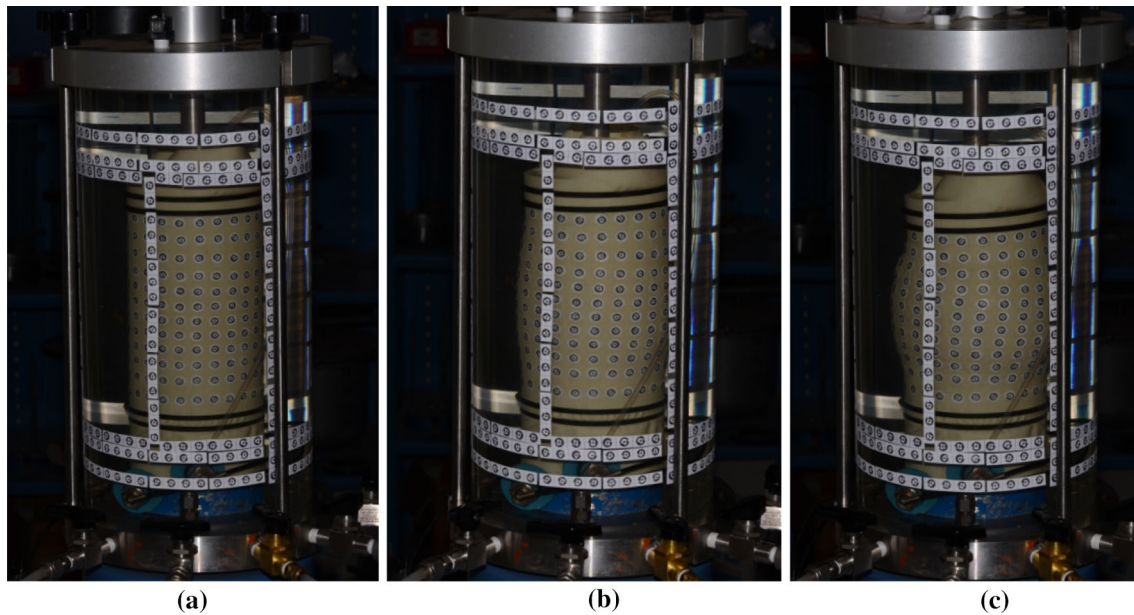


Fig. 10 Soil deformation at different axial displacement levels. **a** 0 mm. **b** 10 mm. **c** 20 mm

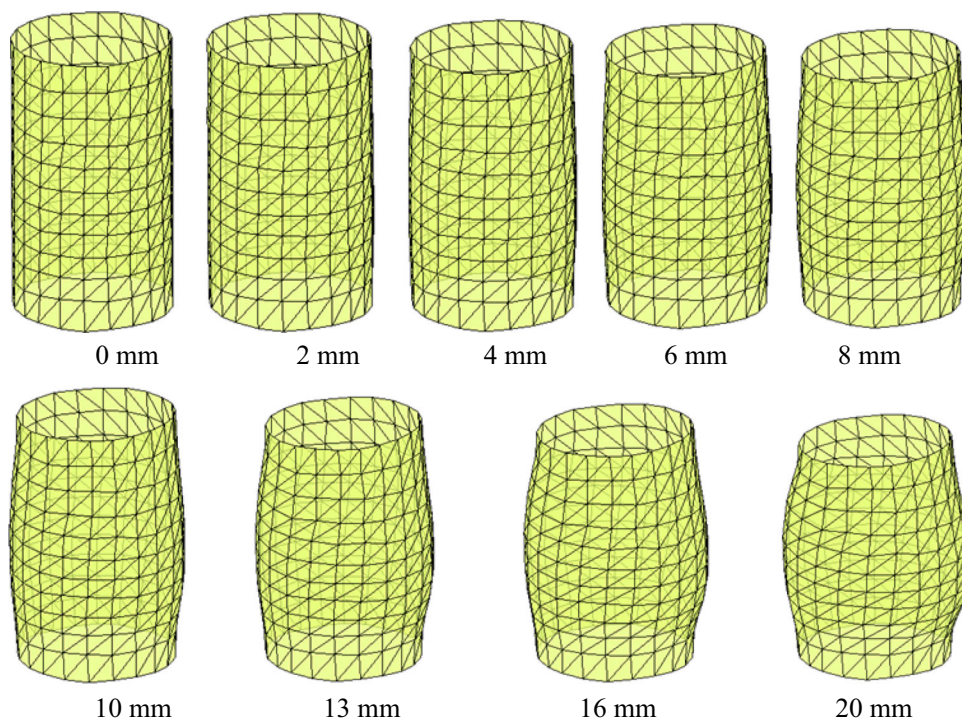


Fig. 11 Triangular mesh at different axial displacement levels

to the use of different meshes. With the 3D coordinates of measurement targets on the soil surface, four triangular meshes using all or part of the targets on soil surface were generated as shown in Fig. 13 for volume change calculation. The total numbers of the measurement targets used for triangular mesh generation were 252, 132, 110, and 88, respectively. The volume change results obtained using

four meshes at different axial displacement levels are summarized in Table 4 and plotted in Fig. 12.

The mean absolute volume change measurement error of four meshes was within 0.16%. However, variations of measurement error did exist among different meshes. The volume change results obtained using meshes A and B with target numbers of 252 and 138 were more close to the

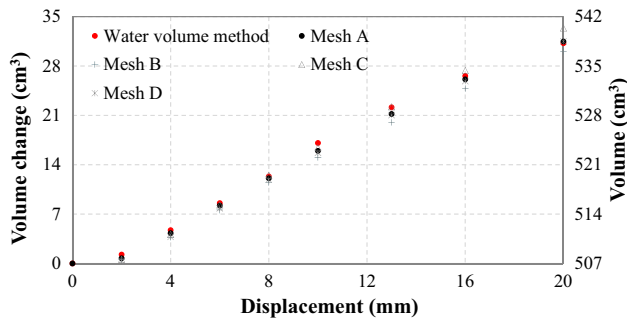


Fig. 12 Comparison of volume changes between the conventional water volume and the photogrammetry-based method

water volume measurement result. Theoretically, the meshes generated using more targets tended to provide more accurate volume measurement results which were consistent with the volume change results summarized in Table 4. In other words, more targets on the soil surface are always beneficial for accurate soil volume/deformation

detection during triaxial testing. This is because the obtained triangular mesh, as typically shown in Fig. 13a, is a better representation of the real soil surface when more targets are used. However, this doesn't necessarily mean the photogrammetry-based method cannot be used when less targets are used. Under this situation, the measurement accuracy can be potentially improved by adopting a different volume calculation or interpolation technique rather than using the triangular mesh obtained through directly connecting adjacent targets with straight lines. Using mesh D as an example, to be more consistent with the real soil shape, different from the triangular mesh, the soil cross section was fitted with a circle using the targets at nearly the same height. In this way, the soil was divided into seven layers. Then, together with the average thickness of each layer, the soil volumes were calculated as summarized in Table 4. With this volume calculation method, using the same 88 targets on soil surface, the overall volume change measurement accuracy was reduced to 0.123% as listed in

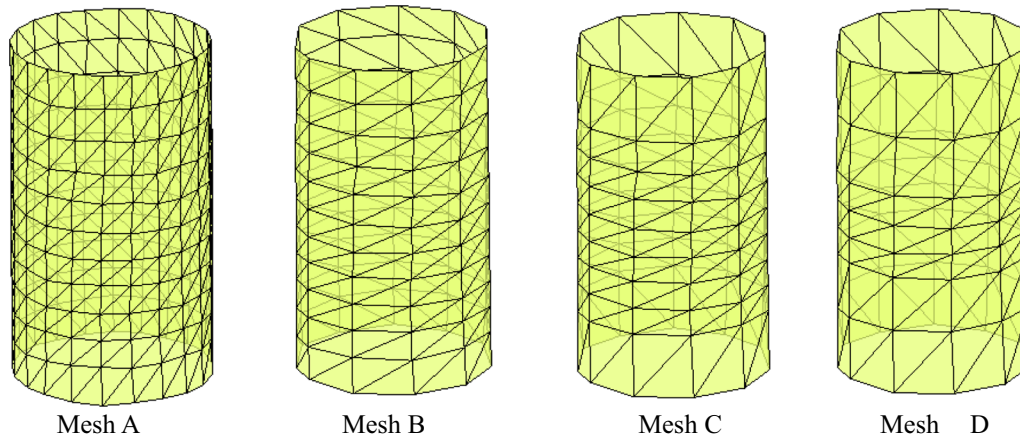


Fig. 13 Volume calculation using different meshes

Table 4 Volume measurement accuracy using different meshes and interpolation techniques

Displacement (cm)	Soil volume (cm ³)	Volume change (cm ³)		Photogrammetry-based method				
		Water volume method		Mesh A	Mesh B	Mesh C	Mesh D	Curved D
0	506.88	0		0	0	0	0	0.00
0.2	508.15	1.27		0.73	0.73	0.6	0.38	0.31
0.4	511.6	4.72		4.31	4.44	4.11	3.78	3.82
0.6	515.44	8.56		8.22	8.59	8.3	7.82	8.03
0.8	519.22	12.34		12.07	12.68	12.53	11.91	12.28
1	523.97	17.09		15.97	16.73	16.4	15.69	16.10
1.3	529.02	22.14		21.19	22.34	22.21	21.04	21.61
1.6	533.47	26.59		26.12	27.39	27.38	25.86	26.53
2	538.12	31.24		31.47	33.04	33.39	31.49	32.33
Mean absolute error	–	–		0.104%	0.103%	0.128%	0.156%	0.123%

column 8 of Table 4 which was better than 0.156% for mesh D. Besides the target number, interpolation technique, and volume calculation method, the volume measurement accuracy can also be influenced by the pattern of the mesh due to the deformation non-uniformity of the soil. That was the reason why the volume measurement accuracies using meshes A and B with different target numbers were very close. Theoretically, under isotropic loading condition, since soil deformation was relatively uniform, fewer measurement targets could be used during triaxial testing with acceptable volume measurement accuracy. However, during triaxial shearing, soil deformation could be significantly non-uniform according to the results presented in [14]. Under this situation, if the soil deformation is axisymmetric, to achieve a high volume measurement accuracy, more targets are suggested to be posted along the axial direction of the soil rather than the circumferential direction. If the soil deformation is neither uniform nor axisymmetric, more targets are suggested to be posted along both the axial and circumferential directions of the soil specimen.

4 Suggestions for accuracy improvement

According to the presented test results, the photogrammetry-based method proved to be accurate for soil volume/deformation measurements during triaxial testing. Theoretically, as long as the triaxial cell wall is accurately reconstructed and the refractive index of the cell wall and confining fluid are accurately known, the accuracy of the photogrammetry-based method is supposed to be equal to 0.01 mm which is considered to be the accuracy of the photogrammetric measurement as reported in [27]. In other words, there is still room to improve the accuracy of the photogrammetry-based method. Several suggestions are listed as follows for this accuracy improvement:

1. The camera used is clearly very important for any photogrammetric measurement. Whether a camera is suitable for photogrammetry measurement depends on several factors (e.g., focal length, image sensor resolution, reliability, and cost). A digital single-lens reflex camera with a fixed focal length lens is recommended.
2. Measurement accuracy is dependent on the camera calibration. Image quality, camera position, and the number of images used can influence the calibration result. Different calibration results will produce different measurement results. The image idealization process, which is required when constructing the optical rays based on the pinhole camera model, requires using the lens distortion parameters, format size, and perspective center location of the image sensor. All these parameters are extracted from the camera calibration. Different camera calibration results can introduce different pixel positions of the measurement targets on the idealized images. Camera orientation results can also be affected by camera calibration results due to the variations in focal length of the lens and format size of the image sensor. As a result, the camera used must be calibrated before the photogrammetric measurement if high measurement accuracy is to be achieved.
3. An assumption of barrel-shaped cell surfaces (i.e., the outer and inner surfaces) is made for the triaxial cell reconstruction. Since the cell wall surfaces are the refractive interfaces, an accurate optical ray tracing highly relies on the representativeness of the barrel-shaped surface. To reduce the error from the optical ray tracing process, a transparent and cylindrical triaxial cell with a uniform thickness is highly recommended. However, when this cell is not available, measurement error during the optical ray tracing process cannot be avoided. To improve the measurement accuracy, this error can potentially be eliminated or at least reduced through calibration. For example, the measurement error distribution pattern can be determined using a rigid cylinder through photogrammetric and photogrammetry-based methods for the exposed in the air and inside of the triaxial chamber conditions, respectively. The obtained error is then subtracted in the photogrammetry-based measurement result. If accurate system parameters such as refractive indices of the confining fluid and cell wall and cell wall thickness are not available, a least-square method can be applied to find the “best” combination of the system parameters by minimizing the differences between the measurement results obtained with and without the triaxial cell conditions.
4. Due to the assumption on the cell wall and its geometrical imperfection, error is introduced to optical ray tracing. This error will be magnified with an increase in the optical ray traveling distance in the triaxial cell. As a result, to increase the measurement accuracy, for the same soil sample, a smaller triaxial cell is always preferred; for the same triaxial cell, a larger soil sample is preferred as long as the soil deformation during testing is not restricted by the cell wall.
5. The refractive index of the confining fluid is an important factor that can significantly influence the volume measurement accuracy as previously discussed. According to the result presented, the overall point measurement accuracy when silicone oil was used as the confining fluid was the better than the water-confined condition. Therefore, silicone oil,

water, or some other transparent liquids, with constant refractive indices under a relatively low pressure range (typically less than 1000 kPa), are recommended to be used as the confining medium. Another benefit of using silicone oil or water as the confining fluid is the obtained images are in better clarity due to the magnification effect of refraction. High-quality images are always beneficial for accuracy of the photogrammetry-based measurements.

6. High-quality images with large depth of field are preferred to minimize the marking error for the photogrammetric analysis and optical ray reconstruction. Therefore, during image capturing, with the built-in flash, the camera used is recommended to be set at a low ISO level (less than 400), small aperture size (F-stop number of 9 or higher), and high shutter speed ($< 1/160$ s). In this way, high-definition images can be captured.
7. The least-square method is used to estimate the 3D coordinates of the measurement targets on the soil surface. To reach high measurement accuracy, more images from different view angles and positions are suggested to be captured. For a single target on the soil surface, at least five optical rays are recommended to be utilized for the least-square estimation.

5 Conclusions

A series of triaxial tests was conducted on an aluminum cylinder with different confining media (i.e., air, water, and silicone oil) and chamber pressure conditions. With the results from these tests, the influences of the assumptions on the triaxial cell wall, cell wall cleanliness, and refractive index of the confining medium on the accuracy of the newly developed photogrammetry-based method were evaluated. Triaxial tests were also performed on a saturated sand specimen to evaluate the influences of number of the targets on soil surface, pattern of the triangular mesh, interpolation technique, and deformation characteristic. Several findings are listed as follows:

1. Since multiple optical rays were used for the measurement of a single point, the measurement accuracy would not be significantly influenced by the obstacles such as cleanliness of the cell wall, the targets on cell surface, the cell frame rods, and the white area caused by camera flash. More images could be captured at different view angles to compensate the missing rays due to the presence of these obstacles without compromising the measurement accuracy.
2. The sensitivity analysis results revealed that the refractive index of the confining medium had the most

significant impact on the overall volume measurement accuracy when comparing with the other two system parameters (i.e., refractive index and thickness of the cell wall). So, the refractive index of the confining medium is recommended to be measured or back-calculated.

3. The validation test on the saturated sand specimen indicated that the volume change measurement accuracy can also be influenced by the number of the measurement targets on the soil surface, pattern of the triangular mesh, interpolation technique, and deformation characteristic of the soil during testing. The triangular mesh, especially for those created using few measurement targets, is not always the best option for the soil volume calculation. Under this situation, the soil volume change accuracy can be improved through an interpolation using those targets.

The point and volume measurement accuracies of the photogrammetry-based method presented in this and previous studies were higher when comparing with the other methods. The presence of the photogrammetry-based method, with the all-around deformation measurement capability, opened a new window for more advanced and in-depth soil behavior characterization (e.g., the relationship between strain localization and soil strength, localized stress–strain relationship for constitutive modeling, and 3D finite element analysis with node by node displacement boundary condition).

References

1. AASHTO (2008) Mechanistic-empirical pavement design guide: a manual of practice. Washington, D.C
2. Alshibli KA, Sture S, Costes NC, Lankton ML, Batiste SN, Swanson RA (2000) Assessment of localized deformations in sand using X-ray computed tomography. *Geotech Test J* 23(3):274–299
3. ASTM Designation: ASTM D7181 (2011) Standard test method for consolidated drained triaxial compression test for soils, Annual Book of ASTM Standards
4. Bhandari AR, Powrie W, Harkness RM (2012) A digital image-based deformation measurement system for triaxial tests. *Geotech Test J* 35(2):209–226
5. Bishop AW, Donald IB (1961) The experimental study of partly saturated soil in the triaxial apparatus. In: Proceedings of the 5th international conference on soils mechanics, Paris, vol 1, pp 13–21
6. Blatz JA, Graham J (2003) Elastic-plastic modeling of unsaturated soil using results from a new triaxial test with controlled suction. *Géotechnique* 53(1):113–122
7. Clayton CRI, Khatrush SA, Bica AVD, Siddique A (1989) The use of Hall effect semiconductors in geotechnical instrumentation. *Geotech Test J* 12(1):69–76
8. Desrues J, Viggiani G (2004) Strain localization in sand: an overview of the experimental results obtained in Grenoble using

- stereophotogrammetry. *Int J Numer Anal Method Geomech* 28(4):279–321
9. Edlén B (1966) The refractive index of air. *Metrologia* 2(2):71
 10. Gachet P, Geiser F, Laloui L, Vulliet L (2007) Automated Digital image processing for volume change measurement in triaxial cells. *Geotech Test J* 30(2):98–103
 11. Helm JD, McNeill SR, Sutton MA (1996) Improved 3D image correlation for surface displacement measurement. *Opt Eng (Bellingham)* 35(7):1911–1920
 12. Li L, Zhang X (2015) A new triaxial testing system for unsaturated soil characterization. *Geotech Test J* 38(6):823–839
 13. Li L, Zhang X (2015) Modified unconfined compression testing system to characterize stress–strain behavior of unsaturated soils at low confining stresses. *Transp Res Record J Transp Res Board* 2510:54–64
 14. Li L, Zhang X, Chen G, Lytton R (2015) Measuring unsaturated soil deformations during triaxial testing using a photogrammetry-based method. *Can Geotech J* 53(3):472–489
 15. Lin H, Penumadu D (2006) Strain localization in combined axial-torsional testing on kaolin clay. *J Eng Mech* 132(5):555–564
 16. Laloui L, Péron H, Geiser F, Rifa'i A, Vulliet L (2006) Advances in volume measurement in unsaturated triaxial tests. *Soils Found* 46(3):341–349
 17. Macari EJ, Parker JK, Costes NC (1997) Measurement of volume changes in triaxial tests using digital imaging techniques. *Geotech Test J* 20(1):103–109
 18. Ng CWW, Zhan LT, Cui YJ (2002) A new simple system for measuring volume changes in unsaturated soils. *Can Geotech J* 39(3):757–764
 19. Owens JC (1967) Optical refractive index of air: dependence on pressure, temperature and composition. *Appl Opt* 6(1):51–59
 20. Richard A, Coffman E, Salazar S, Barnes A (2015) Development of an internal camera-based volume determination system for triaxial testing. *Geotech Test J* 38(4):549–555
 21. Romero E, Facio JA, Lloret A, Gens A, Alonso EE (1997) A new suction and temperature controlled triaxial apparatus. In: *Proceedings of the 14th international conference on soil mechanics and foundation engineering, Hamburg, vol 1, pp 185–188*
 22. Salazar SE, Coffman RA (2015) Consideration of internal board camera optics for triaxial testing applications. *Geotech Test J* 38(1):40–49
 23. Salazar SE, Coffman RA (2015b) Discussion of “A photogrammetry-based method to measure total and local volume changes of unsaturated soils during triaxial testing” by Zhang et al. (<https://doi.org/10.1007/s11440-014-0346-8>). *Acta Geotech* 10(5):693–696
 24. Waxler RM, Weir CE (1963) Effect of pressure and temperature on the refractive indices of benzene, carbon tetrachloride and water. *J Res Nat Bur Stand* 67:163–171
 25. Wheeler SJ (1988) The undrained shear strength of soils containing large gas bubbles. *Géotechnique* 38(3):399–413
 26. White D, Take W, Bolton M (2003) Measuring soil deformation in geotechnical models using digital images and PIV analysis. In: *Proceedings of 10th international conference on computer methods and advances in geomechanics, Tuscon, Ariz., Balkema, Rotterdam, The Netherlands, pp 997–1002*
 27. Zhang X, Li L, Chen G, Lytton R (2015) A photogrammetry-based method to measure total and local volume changes of unsaturated soils during triaxial testing. *Acta Geotech* 10(1):55–82
 28. Zhang X, Li L, Chen G, Lytton R (2015b) Reply to “Discussion of ‘A photogrammetry-based method to measure total and local volume changes of unsaturated soils during triaxial testing’ by Zhang et al. (<https://doi.org/10.1007/s11440-014-0346-8>)” by Salazar and Coffman (<https://doi.org/10.1007/s11440-015-0380-1>). *Acta Geotech* 10(5):697–702

Publisher's Note

Springer Nature remains neutral with regard to jurisdictional claims in published maps and institutional affiliations.